Electron Bernstein emission diagnostic of electron temperature profiles at W7-AS Stellarator

F.Volpe[1], H.P.Laqua, H.J.Hartfuß and the W7-AS Team

Max-Planck-Institut für Plasmaphysik, EURATOM Association
D-85748 Garching, Germany

Abstract

Electron temperature profiles at densities higher than ECE cutoff have been measured by a novel diagnostic based on radiometry of Bernstein-extraordinary-ordinary mode-converted thermal emission of electron Bernstein waves.
The diagnostic has been applied to time- and space-resolved measurements of heat waves, ELMs, L-H transitions and radiative collapses at densities up to $n_e = 3.5 \cdot 10^{20} m^{-3}$.

Introduction

Magnetically confined plasmas do not necessarily fulfill the accessibility criteria for electromagnetic waves in the electron cyclotron (EC) frequency range polarized in the ordinary (O) or extraordinary (X) mode. This may hold especially in high density stellarator plasmas, not affected by the Greenwald limit, and in low magnetic field spherical tokamaks. In such cases the electron Bernstein (B) mode, the third electron cyclotron mode in a *hot* plasma is the "natural" candidate for EC heating, current-drive and diagnostic, since it propagates without upper density limit.
The heating potential of electron Bernstein waves (EBWs) was already demonstrated at W7-AS [1] taking advantage of the O-X-B mode conversion mechanism [4].
The coupling of O and slow X-mode occurs at the cutoff layer for the O-mode: if it is approached with a suitable inclination, defined by $k_y = 0$ and $k_z = \frac{\omega}{c}\frac{\omega_c}{\omega_c+\omega}$ in a frame with z axis along the magnetic field $\mathbf{B}$ and x axis along the density gradient, the two modes coalesce. In the phase space, then, one branch is the prolongation of the other without crossing a region of evanescence ($k_x^2 < 0$). In the physical space this means that 100% of input O-mode energy flows into X-mode and (being unaffected by O-mode cutoff) goes ahead. Then it turns back to the upper hybrid layer where, if $T_e \gtrsim 30eV$, converts completely into the B-mode.
The reversed scheme, BXO, was used at W7-AS for the first spectral measurements of electron Bernstein emission [2]. Since emission reachs blackbody levels, more recently was possible even to measure the first temperature profile [3].
This paper describes the first routinely operating dedicated diagnostic and its results.

Experimental set-up

In the nonaxisymmetric device W7-AS the initial toroidal angle ϕ influences the evolution of the component of EBW refractive index parallel to $\mathbf{B}$, $N_{||}$. A finite $N_{||}$ in the emission region broads the resonance. The high optical thickness for EBWs (a factor c^2/v_{th}^2 greater than ECE), delocalizes the emission to the very outskirt of the broadened resonance layer, any internal emission being reabsorbed. The mentioned Doppler broadening results thus in temperature-dependent, inhomogenous, shift of the spectrum. This undesired spectrum deformation was minimised minimising $N_{||}$ in a

toroidal scan in 3D ray tracing calculations in full stellarator geometry [3].
A gaussian beam focused at the OX conversion layer along the best sightline (best transmittivity and minimal Doppler shift) is collected by an antenna consisting of an ellipsoidal mirror and a corrugated horn.
The beam is focused almost at the diffraction limit because within few centimeters converts in B-Mode and gets high refractive index (perpendicular to **B**), thus diverges much slower than in vacuum, conserving a transverse size similar to that at the waist.
The O-mode polarization detected along the oblique sightline is elliptical, but by $\lambda/4$ phase shift and proper orientation of optical axes it is changed into a linear one by an elliptical waveguide. The phase shift originates from different phase velocity for modes with electric field along elliptical cross-section axes. The broad band $f = 66 - 78GHz$ is covered with a systematic error in phase shift smaller than 10% [3], corresponding to 2% in intensity which can be neglected vs. radiometry errors.
The linearly polarized output is spectrum-analysed in the 70 GHz ECE heterodyne radiometer [5], with 8 extra-channels added for the occasion. Recent coupling with the "zoom" device [6], a 16 narrow filter section with variable intermediate frequency, raises to 48 the total channel number. The Doppler shift for the new antenna is low enough that the EBE spectrum matches the band of the radiometer without necessity to reduce the magnetic field as in [2] or to replace the local oscillator in the radiometer.

Profiles

Fig.1 shows an EBE spectrum in a NBI-heated discharge, rescaled to take into account the transmittivity $< 100\%$. In fact, in spite of antenna optimisation for penetration through a *laminar* cutoff layer, a realistic layer is corrugated and oscillates, therefore locally and transiently can form a non-optimal angle with the ray. By the way the effect is small and a transmittivity $75 - 85\%$ is found, thanks to the short length scale L_n of density profile in the gradient region. Typical W7-AS values of $L_n = 1 - 4cm$ yield in fact effective OX coupling in a cone of aperture $7^0 - 16^0$ around the best direction [1, 3]. Turbulence-induced deviations from the optimal angle are negligible if smaller than this aperture.
The finite $N_{||}$ intrinsic in the oblique detection explains the peculiar shape of the spectrum, characterized by a larger frequency upshift in the center, where the plasma is hotter. As a consequence the high field side of the plasma emits in a narrower band, where most of new channels have been concentrated.

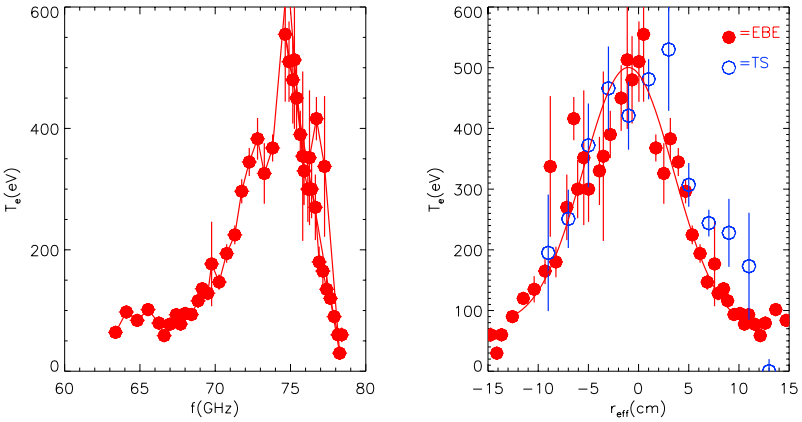

Figure 1: EBE spectrum (left) and profile (right), TS profile

Due to the complicated ray paths and to the shift of emitting layer with respect to the $\omega = \omega_c$ one, the conversion of EBE spectra in profiles is not as straightforward as ECE [3]. Experimental density data and equilibrium code magnetic data are assigned as input to the parallel version of the ray tracing code. This maps the 48 channel frequencies into as many emitting locations in plasma, thus allowing profile reconstruction. Indeed, being the temperature profile also an input for calculations, which involve the

hot dielectric tensor, a "guess" is necessary at the beginning, but in 2-4 iterations the code converges, within error bars, to the definitive profile.
The vertical error bars in the spectrum depend on the precision of the calibration with an hot/cold source, and with some exceptions are of order 10%. Horizontal error bars of $0.5 - 1cm$ in profiles are assigned according to emission region widths computed by the ray tracing code.

Heat waves

The heat wave method has been extended for the first time to overdense plasmas combining EBWs heating and diagnostic.
The plasma cannot be diagnosed and heated at the same harmonic because the heating beam drives a parametric instability at the UHR layer, where the XB conversion occurs. Such instability results in high non-thermal peaks overlapping the thermal spectrum [1].
The problem has been overcome combining EBE measurements at the first harmonic ($66-78GHz$) with EBWs heating at the second harmonic ($140GHz$), modulated in this case with a frequency of $184Hz$.
It should be emphasized that for this the plasma had to be overdense up to the second harmonic O-Mode, i.e. $n_e > 2.4 \cdot 10^{20} m^{-3}$. So high densities are possible at W7-AS after installation of the island divertor [8]. A cross-correlation analysis of EBE channels response to periodic temperature perturbation yields the heat waves amplitudes and phases plotted in fig.2. The two amplitude peaks and delay zeros correspond to off-axis power deposition at $r_{eff} \approx 5cm$ (high β effects as Shafranov shift not yet included in the analysis are expected to remove the systematic $1.5cm$ offset). Heat waves can be recognized in fig.2, propagating from deposition regions inward and outward. The $2ms$ taken to reach the edge, compared to similar ECE-ECRH experiments in underdense limited W7-AS plasma [7], agree with other evidences of good confinement achieved with the island divertor [8].

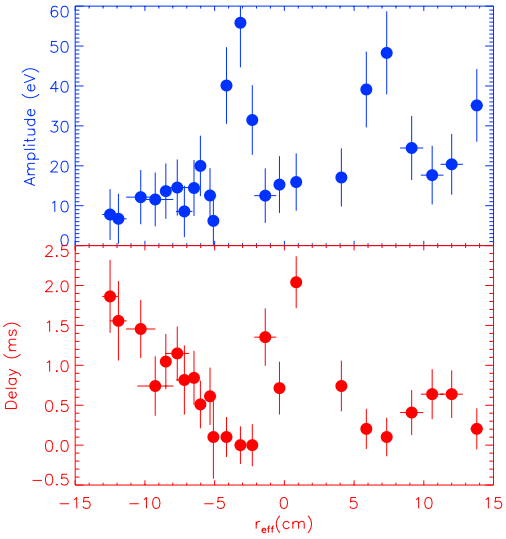

Figure 2: Heat wave amplitude and phase for $n_{e0} = 3 \cdot 10^{20} m^{-3}$

Fast measurements

Innovative applications of EBE diagnostic may concern phenomena occurring at too high density for ECE and over too fast time scales for Thomson scattering.
Examples are L/H mode transitions and ELMs, which at W7-AS often take place at densities out of ECE operational range, $n_e > 1.2 \cdot 10^{20} m^{-3}$ (see fig.1 and 4 in ref.[9]). Fig.3 shows EBE measurements of ELMs at $n_e = 1.4 \cdot 10^{20} m^{-3}$, with $1\mu s$ time resolution. As expected, edge EBE is correlated with H_α, mostly coming from the edge. On the other hand, for any edge temperature spike, the core temperature drops. This is well visible in correspondence with the two biggest spikes in fig.3 and is confirmed for the whole sample by negative correlation with H_α. The time lag for propagation of temperature information from edge to center is $0.4ms$ in the considered discharge with limiter.
Another high density fast phenomenon at W7-AS is the radiative collapse [10]. Fig.4

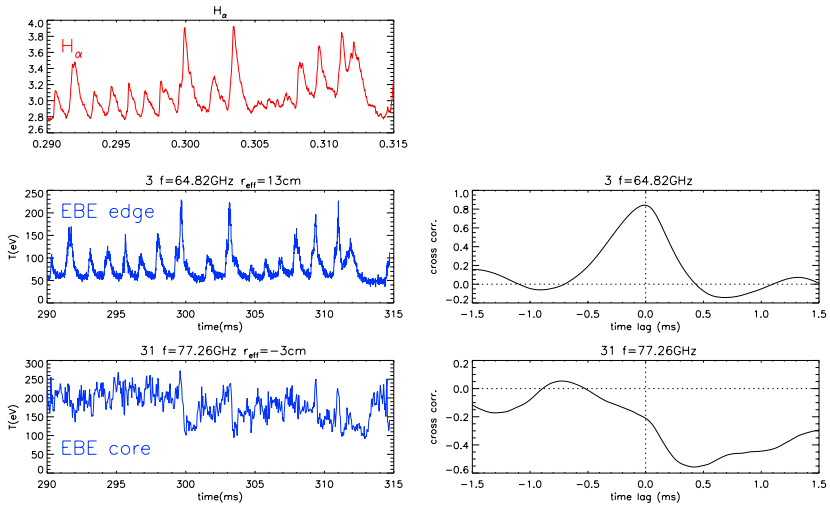

Figure 3: left: ELMs measured by H_α, edge and core EBE; right: EBE-H_α cross-correlations

shows temperature profile oscillations observed by EBE before the definitive collapse. A single collapse is a transition from one stable branch to another of the multistable solution of the time dependent temperature diffusion problem [11].

Observed oscillations can therefore be interpreted as multiple transitions between the two states, like an hysteresis cycle along the S-shaped solution.

Future fields of application could be the high β high density regimes, since EBE time resolution of $1\mu s$ allows comparison with MHD measurements from Mirnov coils and Soft-X diagnostics.

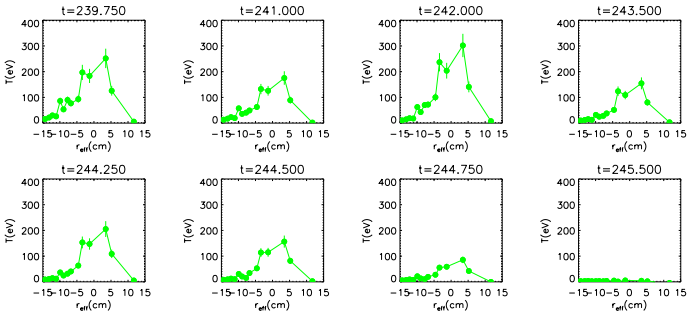

Figure 4: Profile oscillations before radiative collapse, time t in ms

[1]E-mail address: frv@ipp.mpg.de

References

[1] H.P.Laqua *et al.*, Phys.Rev.Lett.**78**, 3467 (1997)
[2] H.P.Laqua, H.J.Hartfuß and the W7-AS Team, Phys.Rev.Lett.**81**, 2060 (1998)
[3] F.Volpe, H.P.Laqua and the W7-AS Team, Proc.27th EPS Conf.Contr.Fusion and Plasma Phys., Budapest, ECA Vol.24B(2000), 1669
[4] J.Preinhaelter and V.Kopecký, J.Plasma Phys.**10**, 1 (1973)
[5] H.J.Hartfuß *et al.*, Proc.6th Joint Workshop on ECE and ECRH, Oxford 1987, p.281; see also H.J.Hartfuß *et al.* Plasma Phys.Control.Fusion **39**, 1693 (1997)
[6] Ch.Fuchs and H.J.Hartfuß, Rev.Sci.Instrum.**72**, 383 (2001)
[7] U.Gasparino *et al.* Plasma Phys.Control.Fusion **40**, 233 (1998)
[8] P.Grigull *et al.*, invited paper nr.17 to this conference
[9] M.Hirsch *at al.*, Plasma Phys.Control.Fusion **42**, A231 (2000)
[10] L.Giannone *et al.*, Plasma Phys.Control.Fusion **42**, 603 (2000)
[11] P.Bachmann et al., Proc.24th EPS Conf.Contr.Fusion and Plasma Phys., Berchtesgaden 1997, p.1817